Jerome Morchain ORCID iD: 0000-0002-3343-5655

The closure issue related to liquid-cell mass transfer and substrate uptake dynamics in biological systems.

Jérôme Morchain[1,5], Vincent Quedeville[1,5], Rodney O. Fox[2,5], Philippe Villedieu[3,4]

1. TBI, Université de Toulouse, CNRS, INRA, INSA, 135 Avenue de Rangueil, 31077 Toulouse, France

2. Department of Chemical and Biological Engineering, Iowa State University, 618 Bissell Road, Ames, Iowa, 50011-1098, USA

3. Institut de Mathématiques de Toulouse, Université de Toulouse, F-31062, Toulouse, France.

4.ONERA/DMPE, Université de Toulouse, F-31055, Toulouse, France.

5. FERMaT, Université de Toulouse, CNRS, INPT, INSA, UPS, Toulouse, France

Abstract

An original dynamic model for substrate uptake under transient conditions is established and used to simulate a variety of biological responses to external perturbations. The actual uptake and growth rates, treated as cell properties, are part of the model variables as well as the substrate concentration at the cell-liquid interface. Several regulatory loops inspired by the structure of the glycolytic chain are considered to establish a set of ordinary differential equations. The uptake rate evolves so as to reach an equilibrium between the cell demand and the environmental supply.

This article has been accepted for publication and undergone full peer review but has not been through the copyediting, typesetting, pagination and proofreading process, which may lead to differences between this version and the Version of Record. Please cite this article as doi: 10.1002/bit.27752.

This model does not contain any of the usual algebraic closure laws relating the instantaneous uptake, growth rates and the substrate concentration, nor does it enforce the continuity of mass fluxes at the liquid-cell interface. However, these relationships are found in the steady-state solution. Previously unexplained experimental observations are well reproduced by this model. Also, the model structure is suitable for further coupling with flux-based metabolic models and fluid-flow equations.

Keywords: Uptake, Regulation, Mass transfer, Bioreactor, Modeling,

1. Introduction

Whatever the approach used to describe bioreactions, one key point is the computation of the mass fluxes between the liquid and biotic phases. This is because bioreactors are essentially multiphase systems and the mass transfer between phases necessarily plays a central role in the definition of the internal bioreaction rates. The interfacial mass-transfer rate, also named uptake rate in microbiology, serves as an input for all bioreaction models including chemically structured and metabolic models (Gombert & Nielsen, 2000; Henson, 2003; Llaneras & Picó, 2008; Nielsen & Villadsen, 1992) and provides upper bounds for the biotransformation rates.

Establishing the relationship between the interfacial exchanges and the variables in the different phases is referred to as a closure problem. Indeed, such relationships are mandatory to obtain a closed system of equations. Henry's law for gas-liquid mass transfer or a drag law for momentum transfer are classical examples, based on more fundamental principles (equality of fugacity or no-slip condition). Thus, a closure law is produced, as a correlation, after solving a subscale problem. This strategy does not conflict with empirical closure laws, based on experimental observations, ignoring the underlying phenomena. In the specific case of bioreactors, a first closure law is needed to express the mass transfer between the liquid and biotic phases from their

respective (bio)chemical composition. A second law relates the growth rate to the uptake rate, through a constant in its simplest form, named biomass yield on substrate. It is generally assumed that the uptake rate is an algebraic function of the substrate concentration in the liquid phase and that it obeys a Monod formalism. The parameters of this law are routinely identified from a fitting of batch and chemostat experimental data. However, this law is unable to predict the actual uptake rate under transient conditions because it is an integral formulation of the closure issue: an implicit hypothesis of quasi steady state for the biotic phase is attached to this law and limits the validity of the mathematical model to cases where the biological phase evolves through a succession of equilibrium stages. Much experimental evidence of the inapplicability of this equilibrium law under transient conditions has been presented over the past decades (Pickett et al., 1979; Silveston et al., 2008). Several authors proposed modified forms for the uptake rate, including static approaches such as a metabolic excess contribution (Xiu et al., 1998), or a dynamic approach involving a differential equation for the uptake rate (Lambert & Kussell, 2014; Sonnleitner & Käppeli, 1986; Sweere et al., 1988). The dynamic approach decouples the uptake rate from the substrate concentration in the medium but despite this improvement, the model proved unable to reflect the transient response in terms of both growth and uptake rates (Sonnleitner, 1998; Sweere et al., 1988). This suggests that the second closure law present in these models, i.e., an algebraic link between uptake and growth rate, is incorrect. Other dynamic models focused on the growth rate as the central variable of the model (Morchain & Fonade, 2009; Young et al., 1970) from which the uptake rate is deduced. It can be concluded from those studies that the relationship between uptake and growth rate under transient conditions (namely the second closure law) is a central point in bioreactor modeling and deserves more attention.

Notwithstanding, care must be taken to limit the number of biological-phase internal variables in order to preserve the trackability of the model. In this context dealing with rates or fluxes appears as an interesting alternative to concentration/kinetic models (Pigou, 2018; Pigou & Morchain, 2015).

As in any multiphase reactive system, the uptake rate must be considered along with the mass transfer of species at the interface, or here specifically the transport of nutrients toward the cell membrane (Linkès et al., 2012; Merchuk & Asenjo, 1995; Siebler et al., 2019). Also, the concept of physical or biological regimes, borrowed from chemical engineering, have been adapted to biological system (Morchain, 2017; Morchain et al., 2017; Sweere et al., 1987). In previous works, this question was addressed through a 1-D diffusion transport equation in a spherical domain surrounding a fictitious spherical cell. Blackman (bi-linear) and Michaelis-Menten formulations for the uptake law were tested and metabolic consequences of uptake rate fluctuations were addressed (Linkès et al., 2012, 2014). But in both articles, it was considered that the cell microenvironment fluctuates while the uptake capacity remains constant. Moreover, the employed numerical techniques were time consuming and both the spatial and temporal ranges where limited.

Here, we propose a multiscale model, formulated at the reactor scale, including the substrate transport toward the cell surface, the substrate uptake, the regulation of the uptake system, and the adaptation of the cell growth rate capacity. The last two aspects constitute the improvement with respect to previous works in the sense that we do not refer to static closure laws anymore and propose instead a dynamic model for the specific growth and uptake capacities. After presenting the dynamic model formulation and its heuristic foundation, the steady-state solution is proposed showing that the usual closure laws between the substrate concentration, the uptake and growth

rates emerge as steady-state outputs of the dynamic model. Then, numerical experiments in transient situations are provided to further enlighten the salient features of the model. A variety of responses, consistent with previously published experimental results, are obtained depending on the ratio of the characteristic time scales of the regulatory mechanisms. In particular, the model is shown to behave properly in the case of external mass-transfer limitation, which is an important property in view of coupling this dynamic biological model with fluid flow models (typically Computational Fluid Dynamics or Compartment Model Approach) for industrial applications.

2. Multiscale model for biological reactors

2.1. Standard static model

In the most classical and simple model, the mass balances for the biomass concentration, $X(g_X.L^{-1})$, and the substrate concentration, S $(g_S.L^{-1})$, in a spatially homogeneous open reactor characterized by its dilution rate D (h^{-1}), reads:

$$\frac{dX}{dt} = (\mu_{st} - D\ )X \tag{1}$$

$$\frac{dS}{dt} = D\left(S_f - S\right) - \frac{1}{V}\int_{\Omega}\ \varphi\ d\omega = D\left(S_f - S\right) - q_S X \tag{2}$$

In equation (2), we first choose to express the sink term as the integral of the mass flux density $\varphi\ (kg.m^{-2}.s^{-1})$ over the liquid-cells total boundary $\Omega\ (\mathrm{m}^2)$ in the volume V (m^3). Conveniently, this sink term is generally rewritten as a specific consumption rate, q_S $(g_S.g_X.h^{-1})$, multiplied by the mass of cell per unit volume, X. It remains that it is a rewriting of an interfacial mass-transfer term.

This system of equations remains unclosed until closure laws for the specific growth rate, μ, and the specific uptake rate q_S are prescribed.

$$q_S = q_{S,max}\frac{S}{k_S+S} \tag{3}$$

$$\mu_{st} = Y_{SX} q_S \quad (4)$$

In these equations, S_f $(g_S.L^{-1})$ is the sugar concentration in the feed, Y_{SX} is the substrate into biomass conversion yield $(g_X.g_S^{-1})$, μ_{st} is the static specific growth rate (based on local concentrations), $q_{S,max}$ is the maximum substrate uptake rate $(g_S.g_X^{-1}.h^{-1})$ and k_S $(g_S.L^{-1})$ is the affinity constant of the enzymatic transport system involved at the cell membrane. The properties of the uptake system are assumed to be known from batch and chemostat cultures. As a consequence, both the specific growth and uptake rates are expressed as algebraic functions of the substrate concentration identified under balanced growth conditions.

2.2 Multiscale dynamic model

In the dynamic model, we introduce three additional variables: the growth capacity, μ, the uptake capacity, ϕ, and the substrate concentration at the liquid-cell interface, S_{int}. Growth and sugar uptake capacities are now time-dependent variables defining, at any time, the current upper limits for the corresponding specific rates. The vocabulary is here borrowed from Sonnleitner (Sonnleitner et al., 1997; Sonnleitner & Hahnemann, 1994; Sonnleitner & Käppeli, 1986). Thus, a clear distinction must be made between the current cell capacities and the actual uptake or growth rates. This crucial point is reflected in the notation: cell capacities are referred to as μ^b and ϕ whereas the actual uptake rates are noted with a superscript *a* for *actual*. The originality resides in the decoupling of uptake and growth rates from the bulk substrate concentration. Moreover, uptake and growth rates are also uncoupled.

The model consists in two conservation equations for the total biomass and substrate concentrations in a volume of control, two equations describing the dynamics of internal cell properties and one equation for the substrate concentration at the cell-liquid interface. The original point is that growth and uptake rates are not

calculated as algebraic functions of the substrate concentration. Both are time-dependent cell properties exhibiting their own adaptation rate, as shown in equations (7) and (8).

$$\frac{dX}{dt} = (\mu^a - D\ )X \tag{5}$$

$$\frac{dS}{dt} = D\left(S_f - S\ \right) - \phi^a X \tag{6}$$

$$\frac{d\phi}{dt} = \frac{1}{\tau_{\phi,in}}\left(\frac{\mu}{Y_{SX}} - \phi\right) + \frac{1}{\tau_{\phi,ex}}\left(q_{S,max}\frac{S_{int}}{k_S + S_{int}} - \phi\right) \tag{7}$$

$$\frac{d\mu}{dt} = \mathrm{r}(\mu, \phi^{\mathrm{a}})(\phi^a Y_{SX} - \mu) \tag{8}$$

$$\frac{dS_{int}}{dt} = \frac{1}{\tau_m}(S - S_{int}) - \phi^a X \tag{9}$$

S_{int} is the substrate concentration at the liquid-cell interface obtained from a mass balance at liquid-cell interface (9) considering transport from the bulk and uptake. τ_m is the characteristic time of micromixing responsible for the transport of substrate to the cell membrane, $\tau_{\phi,in}$ is the characteristic time of uptake capacity adaptation driven by the substrate demand for growth (internal demand), $\tau_{\phi,ex}$ is the characteristic time of uptake capacity adaptation induced by the substrate availability (external supply). Three additional relationships allow for the actual uptake and growth-rate calculation, considering physical and biological regimes.

$$\phi^a = \min(\phi, \frac{S}{X\tau_m}) \tag{10}$$

$$\mu^a = \min(\mu\ , Y_{SX}\phi^a) \tag{11}$$

$$r(\mu, \phi^a) = \begin{cases} \frac{1}{\tau_\mu} + \mu \; if \; Y_{SX}\phi^a - \mu > 0 \\ \mu \; if \; Y_{SX}\phi^a - \mu < 0 \end{cases} \quad (12)$$

τ_μ is the characteristic time of cell growth capacity adaptation (Morchain & Fonade, 2009).

External mass transfer, uptake and growth occur in series and this encourages the use of the limiting rate concept, which leads to expressions (10) and (11). Equation (10) distinguishes uptake in the physical or biological regime: it states that the actual uptake rate, ϕ^a, is either determined by the cell current uptake capacity, ϕ, or by the maximum rate of mass transport to the cell (Morchain et al., 2017). If the external transport of substrate is sufficient, the actual substrate uptake rate, ϕ^a, coincides with the current uptake capacity, ϕ, of the microorganism. In the opposite situation, the actual substrate uptake rate might be eventually upper bounded by the external mass flux. The maximum value of this upper bound is obtained through $\frac{1}{\tau_m}(S - S_{int})$ in the limit of S_{int} going to zero. Equation (11) indicates that the actual growth rate is either set by the cell growth capacity, μ, or by the actual glucose uptake rate ϕ^a. Equation (12) describes the rate of specific growth rate adaptation inspired by a previous works (Morchain & Fonade, 2009; V. Quedeville et al., 2018). In the present version, the cell demand is estimated from the current growth capacity and compared to the actual uptake rate to dynamically adapt the cell growth capacity. Also, Y_{SX} is not used to set μ from ϕ^a but to decide whether the growth capacity can be increased or not, considering the actual uptake rate.

All together, these features lead to a coupled multiphase and multiscale dynamic model of a bioreactor accounting for different possible limitations. Examination of the

steady-state and dynamic behaviors of this model are provided hereinafter with a view of identifying the magnitude of the different time scales introduced. Note that a simplified version assuming $\tau_{\phi,ex} = \tau_{\phi,in}$ is provided in Appendix A. There is no reason for these constants to be identical in all situations but we let some degree of liberty by using two distinct parameters. It proved that sensible results are obtained when parameter values are similar.

3. Results

3.1. In biological systems the flux balance at the interface only holds at steady state

The steady-state solution to the problem is obtained by setting all time derivatives equal to zero. Details are provided in Supplementary Information. Focusing on equation (7) it appears that both terms must be equally zero at steady state and equation (9) entails that the actual uptake rate will equal the external mass transfer rate. It follows that, at steady state, the transfer, uptake and utilization rates are balanced. Although the last statement may appear as trivial, being a fundamental law of biology, it comes out, in our modeling approach, as a property of any biological system at steady state and results from the introduction of the interfacial concentration at the cell-liquid interface. However, transport and uptake mass fluxes at the cell-liquid interface are not balanced under transient conditions as illustrated in the following. Note that the steady-state solution of the dynamic model is identical to that of the static model in the limit of τ_m going to zero (perfect micromixing). Also, the substrate uptake and growth rates are proportional at steady state. Here this steady-state ratio was considered as constant, without ignoring possible dependence on the growth rate and a maintenance term (Bailey & Ollis, 1986; Maluta et al., 2020).

3.2 Numerical studies of transient cases

The set of dynamic equations was solved using a second-order explicit Runge-Kutta method. The time step is set to $5\,10^{-6}\,h$ which proves to be sufficiently small, considering the dynamics of the different processes involved, to get converged numerical results. The values of the constants and parameters are presented in Table 1.

The batch case:

An illustration of the time evolution of the dynamic variables in a batch culture is provided in Figure 1. Initial conditions are $\{X = 0.1; S = 10; \mu = 0.5; \phi = 1; S_{int} = 10\}$ and the time constants are $\tau_m = 1.4\,10^{-4}\,h, \tau_{\phi,in} = \tau_{\phi,ex} = 0.1\,h, \tau_\mu = 1\,h$. The time profiles of biomass and substrate concentrations are consistent with expectations (Figure 1a, 1b). Substrate exhaustion takes place at $t = 4.5\,h$. Until that point, the specific growth rate, Figure 1c, rose from its initial value ($0.5\,h^{-1}$) towards a maximum value ($Y_{SX}\phi^a = Y_{SX}q_{S,max} = 1\,h^{-1}$) following a pseudo-first-order dynamics (see equations (8) and (12)). By this time, the uptake capacity, Figure 1d, jumps quickly from its initial value ($1\,g_S.g_X^{-1}.h^{-1}$) to 1.5 due to high availability of substrate, and then increases more slowly, following the dynamics of the specific growth rate. This time profile is consistent with the two terms in equation (7). In the present case, the uptake rate never exceeds the rate of external transport, so the interfacial concentration remains equal to the bulk concentration ($S/S_{int} = 1$) as seen in Figure 1e. The two differences reported in Figure 1f quantify the imbalances between:

i. environmental supply and the cell uptake capacity $q_S - \phi$

ii. cell demand for growth and the cell uptake capacity, $\mu/Y_{SX} - \phi$

This figure reveals that equilibrium or *balanced growth* was reached before substrate exhaustion as far as the uptake capacity, ϕ, simultaneously approached the

environmental supply (quantified by q_S) and the cell demand (quantified by μ/Y_{SX}). Once glucose is depleted, growth stops, the actual growth and uptake rates decrease to zero immediately, while the corresponding capacities relax toward zero according to the related time constant by following a first-order decay. The exhaustion of glucose creates a significant imbalance between the cells' demand and the environmental supply. It does not imply that the uptake capacity has vanished whilst growth is obviously not permitted anymore.

The route toward the steady state in a chemostat mode:

The second test case consists of the convergence towards a steady state. The substrate concentration in the feed is set to $S_f = 10 g_S.L^{-1}$and the dilution rate to $D = 0.4\ h^{-1}$. The vector of initial values is $\{X = 2; S = 0.1; \mu = 0.5; \phi = 0.8; S_{int} = 0.1\}$. All parameters are identical to those used for the batch case, except $\tau_{\phi,in} = 2\,\tau_{\phi,ex} = 0.02\ h$. Results are presented in Figure 2.

The final biomass concentration goes to $5\ g_X.L^{-1}$ which corresponds to $(S_f - \bar{S})Y_{SX} \approx S_f Y_{SX}$. The cell growth rate goes to $\bar{\mu} = D = 0.4\ h^{-1}$, as expected, and the uptake rate, along with the uptake capacity, goes to twice this value $\bar{\phi} = 0.8\ g_S.g_X^{-1}h^{-1}$, in agreement with the definition and value of Y_{SX}. It is further observed, considering the value of the interfacial concentration $\overline{S_{int}} \approx 6.664\ 10^{-3} g_{XS}.L^{-1}$, that $\overline{q_S} = q_{S,max}\ \frac{\overline{S_{int}}}{k_S + \overline{S_{int}}} = 0.79979\ g_S.g_X^{-1}h^{-1}$. Consequently, the mass balances are accurately satisfied at steady state.

As far as the dynamics are concerned, glucose accumulates as long as both the cell concentration and the growth rate are low ($t < 0.6\ h$). Then, the cell concentration, the specific growth and uptake rates keep increasing while the glucose concentration decreases rapidly until $t = 1.45\ h$. Indeed, the biological demand exceeds the total

sugar feed rate at the reactor scale and this causes a rapid fall-off of the total mass of substrate in the reactor with no impact, for the moment, on the uptake rate (Figure 2b, 2d). From $t = 1.45\ h$ onward, the regime changes from biological to physical. This shift between the two regimes is clearly evidenced in the glucose flux imbalance curve (Figure 2f). The beginning of the cultivation was characterized by a q_S much larger than the cell uptake capacity, while the substrate uptake rate itself exceeded the substrate demand for growth (μ/Y_{SX}). Hence two signals were perceived by the biological phase: the uptake capacity can be augmented and the growth rate can also be increased. This feast period supports the exponential growth of the population and a proportional increase of the overall substrate consumption. In a chemostat where the substrate supply is $D.S_f$, this exponential growth is not sustainable. At some point, the drop in the substrate concentration induces a sudden drop in the external mass-transfer rate. The interfacial substrate concentration starts decreasing and this acts as a signal to the cells that the environment is getting depleted (Figure 2e). It is crucial to understand here that a decrease in the interfacial concentration is both the consequence of the actual uptake rate being greater than the external mass-transfer rate and the starting point of the uptake regulation. In our model, the information is passed to the regulatory system through the concomitant drop in $q_S(S_{int})$. According to the second term in equation (7), the uptake capacity starts decreasing.

We considered here that the response to external changes is fast, so the uptake capacity decreases rapidly in the wake of the interfacial concentration. Thus, the reduced actual uptake rate instantaneously impacts the actual growth rate (Figure 2c and 2d). The prolonged decrease of the uptake rate finally allows a higher interfacial concentration to be reached. It can be observed that the two regulatory mechanisms

controlling the evolution of the uptake capacity lead to a second-order-like response in terms of the interfacial concentration.

The dynamic response to an upshift in the dilution rate:

The change in the dilution rate forces the cell population to increase its growth rate in the long term while causing, from the cells' point of view, a sudden and unpredictable increase in the substrate concentration in the short term. It is generally observed in that case that the growth and uptake rates are no longer proportional to one another and neither of them is any longer algebraically related to the substrate concentration. A dilution rate upshift from 0.25 to $0.5\ h^{-1}$ is thus imposed to a culture previously set at steady state through a long-running simulation at $D = 0.25\ h^{-1}$ with $S_f = 5 g_S.L^{-1}$. Various combinations of characteristic times are tested and the results compared. Simulations are performed with two identical characteristic times (dark to light blue curves) or a faster adaptation to the external concentration (dark red to orange). Lighter colors coincide with the smallest characteristic times (fastest adaptation). As expected, unphysical results were obtained if $\tau_{\phi,ex} > \tau_{\phi,in}$ and these simulations are not presented. Indeed, in those cases, the uptake regulation would be more sensitive to the cells' demand than to the external changes. Also, the whole dynamics would be imposed by the time constant for growth-rate adaptation and the causality between a cascade of events (changes in concentration, inducing uptake and finally growth adaptation) would be violated. For the same reason, both the characteristic times of uptake regulation are smaller than the characteristic time of growth-rate adaptation. The investigated combinations of time constants respect the following rule:

$$\tau_{\phi,ex} \leq \tau_{\phi,in} \ll \tau_{\mu} \quad (13)$$

Figure 3a presents the responses in terms of substrate and biomass concentrations for different combinations of characteristic times. The dynamics of uptake regulation have little to no impact on the biomass concentration whereas the substrate concentration is strongly affected. This result is readily explained by the larger time constant of growth-rate adaptation. Biomass concentration first slightly decreases from 2.5 to 2.25 $g_X.L^{-1}$ because the dilution rate exceeds the growth rate, then the inverse situation takes place over the time scale of growth-rate adaptation (hours). Smooth or oscillating responses are obtained depending on the value of the time constants and this variety of responses is, as such, very interesting. In general, smooth concentration profiles are obtained if the uptake regulation responds very quickly to the external concentration (orange and light-blue curves).

Our model connects the two specific rates through differential equations and their interdependencies are illustrated in Figure 3b. The uptake capacity, in dashed lines, lies between the substrate demand for growth, $\frac{\mu}{Y_{SX}}$, and the external supply $q_S(S_{int})$. The dynamics of μ is only slightly dependent on the uptake regulation because of the timescale separation already reported. Thus, the cell demand, $\frac{\mu}{Y_{SX}}$, evolves from 0.25/0.5 to 0.5/0.5 following a pseudo-first-order trend. The external supply, $q_S(S_{int})$, is highly dependent on both the mixing efficiency and the uptake regulation through equation (9). The ratio between the characteristic times defines how close the ϕ curves are to the $q_S(S_{int})$ curves. The orange curves reveal that when $\tau_{\phi,ex} \ll \tau_{\phi,in} \ll \tau_{\mu}$, the uptake capacity is always close to the local equilibrium value $q_S(S_{int})$

and the uptake rate can therefore be said "at equilibrium" with the environment. Here, the equilibrium law, $q_S(S_{int})$, strictly valid only at steady state, would constitute a fair approximation of the actual uptake rate. In other situations, both the internal demand and the external supply contribute to the evolution of the uptake capacity. Focusing again on the dark-blue curves, one observes that the uptake capacity more than doubles within the first 15 minutes (from 0.5 to 1.1 $g_S.g_X.h^{-1}$) in response to the accumulation of glucose. The substrate consumption rate at the reactor scale, $\phi^a.X$, now largely exceeds the hydraulic term $D(S_f - S)$ and thus causes a rapid drop in the substrate concentration, further reflected by a drop in $q_S(S_{int})$ inducing in turn a decrease in ϕ around 15-20 minutes. In the following 90 minutes, the uptake capacity keeps increasing, driven by a constantly increasing demand μ/Y_{SX}. The cell demand itself increases because the uptake rate is larger than the consumption rate associated with growth, as expressed in equation (8). In the meantime, the cell concentration keeps decreasing since μ remains lower than D. In the end, the overall substrate consumption rate at the reactor scale, $\phi^a.X$, is almost constant and only slightly superior to the hydraulic term, which explains the linear decrease of the substrate concentration curve.

Since the overall consumption rate exceeds the feed rate, one reaches that point where the residual concentration is so low that neither the cell demand nor the uptake capacity can be satisfied any longer. This happens around $t = 2.3\,h$, and it is evidenced by the inversion of the relative position of the $q_S(S_{int})$ and μ/Y_{SX} curves with respect to ϕ. In the long term this ensures that the biological system will reach a steady state.

Response to a sudden substrate exhaustion:

This experiment reflects what occurs, in multistage bioreactors or in large-scale bioreactors, when cells are transported from a highly concentrated zone to a substrate depleted zone. In this numerical experiment, the feed concentration of a chemostat operated at $D = 0.5\ h^{-1}$ initially fed at $S_f = 10\ g_S.L^{-1}$, is suddenly lowered by half. The characteristic times are $\tau_{\phi,ex} = \tau_{\phi,in} = 0.1\ h, \tau_\mu = 1\ h$. Results are presented in Figure 4.

It is remarkable that the substrate concentration drops down from its initial value ($S \approx 0.01\ g.L^{-1}$) to a small positive value while the interfacial concentration falls to zero. The cells thus exhaust their immediate environment but this does not mean that the actual uptake rate goes also to zero. In fact, the actual uptake rate is now limited by the external mass-transfer rate and falls well below the uptake capacity of the cell. This possibility to describe a positive uptake rate at zero interfacial concentration is an important feature of the model issued from the flux formulation. Prior to the perturbation, uptake and growth rate were at equilibrium. As far as uptake is now limited, growth is also affected by virtue of relationship (11). As a result, the actual growth rate is much lower than the growth capacity and it is also much lower than the dilution rate leading to the wash-out of cells. This decrease in the cell concentration explains why the actual (specific) uptake rate first drops down and then increases in the first instant following the perturbation whilst both the bulk and interfacial concentrations remain constant. This behavior is a consequence of relationship (10). In this aspect, the model predicts a non-intuitive change in the specific uptake rate occurring in a time period where the concentrations are steady. During that period of time, the specific uptake rate evolves not because of a higher amount of substrate available but due to the decrease in the biomass content of the

reactor. Fewer cells being present and their specific uptake rate being limited, the overall substrate consumption decreases and becomes eventually smaller that the substrate inflow, which entails an accumulation of substrate in the reactor from $t > 0.2h$ onward.

During the entire time window of the simulation presented here, the substrate demand for growth is far above the supply from the environment and one can figure out that this signal would trigger the consumption of internal storage compounds. Hence, we observe that this model can also help to further address the issue of predicting the changes in the amount of storage compounds because it provides quantitative information regarding the difference between the cells' needs and the actual supply from the environment.

3.3 Comparison to experimental data

The dilution rate upshift ((Sonnleitner et al., 1997)*:*

We reproduced the dilution rate upshift experiment of Sonnleitner and co-workers. The comparison of our fitted model with these experimental data is presented in Figure 5 while details are provided in Appendix B. A reasonable agreement between the experimental data and our model predictions is obtained. Interestingly none of the modeling approaches of these authors could reproduce the 30 minutes bump followed by a quasi-linear concentration decrease during the next 90 minutes. The static closure law between uptake and growth rates, introduced through equation 8 in their seminal article (Sonnleitner & Käppeli, 1986) is responsible for that failure.

Response to repetitive substrate perturbations:

The uptake kinetics in yeasts exposed to repetitive glucose pulses was studied using dynamic 13C-tracing by Suarez-Mendez and co-workers (Suarez-Mendez et al.,

2017). A continuous cultivation at $D = 0.1\ h^{-1}$ was performed first with a constant feed then with an intermittent addition of glucose for 20 s every 400 s. The feed flow and the concentration during the addition were adjusted to ensure the same averaged glucose feed rate as in the continuous feeding mode. The periodic feed was prolonged over 500 cycles to ensure that a stationary state is reached. The glucose concentration in the medium was measured as well as intracellular metabolites of the glycolytic chain. We first reproduced this experimental procedure with our model using the same set of parameters as for the Sonnleitner's experiment simulation. The results presented in Figure 6a indicate that the effect of a periodic feed on substrate uptake dynamics is well reproduced with our model (at least for a yeast). The consumption of the added glucose is completed in the 280 seconds following the 20 s addition. We further observed that any combination of parameters leading to $\frac{q_{S,max}}{k_S} \approx 7$ with k_S larger than the mean concentration is suitable to fit the data since it provides a good estimate of the slope of the experimental $q_S = f(S)$ as shown in figure 6b. However, the time evolution of the experimental uptake rate suggests that instantaneous uptake is controlled by a diffusion driven process. Nonetheless, our model filters this dynamic ($\tau_{\phi,in}$, $\tau_{\phi,ex}$ $\approx$ feed cycle duration) and provides, through ϕ^a, a good estimate of the mean uptake rate during the cycle. Interestingly, when a periodic feed regime is imposed, the mean uptake capacity is larger than the mean actual uptake whereas both rates are strictly equal if steady conditions are imposed. A similar observation is reported by the authors of the experimental study (Suarez-Mendez et al., 2017).

4. Discussion

The uptake rate in biological systems is not an algebraic function of the interfacial concentration (in the mathematical sense) but the solution of a problem involving the

interfacial concentration. This is a subtle but fundamental distinction. In multiphase chemical reactors, the interfacial concentration appears at some point in the modeling but can further be eliminated considering the continuity of mass fluxes at the interface along with a thermodynamic law of equilibrium or a reaction rate expressed as a true mathematical function of the interfacial concentration that is valid on any time scale. Thus, in chemical systems it can be assumed that reaching the equilibrium at the interface is faster than any other processes. Such an assumption is conceptually irrelevant for biological systems. Indeed, the essential feature of biological systems is the ability to adapt their demand to the external supply, but this is never instantaneous. As a result, the steady-state correlation between the substrate concentration and the actual uptake rate should not be used as a closure law to calculate the magnitude of mass transfer between phases under any circumstances (in transient regimes). In this work, we assumed that the steady-state correlation obeys a Michaelis-Menten formalism; its parameter being identified from a series of continuous culture in chemostat at various dilution rates. We used this steady-state correlation as an attractor for the uptake capacity (second term on the right-hand side of equation (7)). In biological systems the uptake rate is also dependent on the cell uptake capacity, which is dynamically updated to reconcile the cell demand and the external supply. Thus, the interfacial concentration is part of the problem solution but it is not sufficient to close the problem.

Considering the cell uptake capacity as a cell property, along with the fact that this capacity may not be realized in case of external mass-transfer limitation, is a change of paradigm. In other words, the cells uptake substrate at a rate matching their needs irrespective of the actual substrate concentration. The causality is such that the concentration results from the uptake. It is inconsistent to impose the uptake rate from

the concentration as clearly evidenced through the fact that the uptake rate can be positive while the interfacial concentration is zero. In this context, equation (10) states that the uptake rate is as high as the cell can currently do (equals the current uptake capacity, ϕ) on condition that the external mass transfer is not limiting. Clearly the local maximum uptake rate ϕ differs from the absolute maximum uptake rate $q_{S,max}$. Thus, the availability of substrate does not imply that the uptake is at the maximum rate and conversely, the exhaustion of substrate at the cell surface does not imply a null uptake rate. This argues for a reexamination of the concept of limiting and excess concentration, with respect to the cell needs rather than in an absolute way.

Adopting the cell's point of view requires the introduction of the interfacial concentration in the model. If it is exact that, in a well-micromixed bioreactor, S can be substituted to S_{int} with no impact on the numerical calculation, such a substitution masks the role of the interfacial concentration as a signal involved in the regulation of the uptake rate (present in equation (7) and evidenced experimentally in (Youk & van Oudenaarden, 2009), fig4a). A correlation between the uptake rate and the concentration at the liquid-cell interface is found at steady state. Such a correlation emerges *as a property of the system at steady state* in accordance with the experimental observations, but the transient uptake rate does not follow this "equilibrium law". Illustration of this fact is provided in Figure 7 in the form of dynamic phase portraits (Palsson, 2011) for three situations investigated in this work. Trajectories located below the steady-state line reflect that the cell properties are controlling the rate of reaction (biological regime), while trajectories located above this line indicate that reactions are controlled by an external mass-transfer limitation.

As far as regulation is concerned, the model involves three loops combining intracellular steps (dashed lines) and external steps (continuous lines) as shown in

Figure 8. The positive feedback loop connecting ϕ and μ, which could generate system instability, is globally constrained since it is nested in a slow negative feedback loop involving the substrate and biomass concentrations, and preceded by another faster negative feedback loop involving the substrate concentration only. It was already mentioned that nesting positive and negative feedback loops is common in biological systems and presents advantages in terms of stability and noise filtering (Brandman et al., 2005).

The model is inspired by the structure and regulations of the glycolytic chain present in any living organism whilst different biomolecules are involved depending on the organism. In *S. cerevisiae*, the upper and lower glycolysis pathways are connected at the FBP (Fructose-1,6 biphosphate), GAP (Glyceraldehyde3-Phosphate), DHAP (DiHydroAcetone Phosphate) node, as illustrated in (van Heerden et al., 2014). At equilibrium, the fluxes in the upper and lower parts are equal (translated into $q_S = \phi = \mu/Y_{SX}$ in our model). A consequence, among others, of a too massive influx is the accumulation of all compounds in the upper glycolysis (Suarez-Mendez et al., 2017). Interestingly, the accumulation of the end product, FBP, promotes an increase in the rate of the reaction converting phosphoenolpyruvate into pyruvate within the lower glycolysis. This can be regarded as a way to improve the carbon processing capacity of the lower glycolysis pathway (direct sense of the green loop). In the meantime, the accumulation of G6P (another compound of the upper glycolysis) amplifies the accumulation of intracellular glucose which, in the end, negatively impacts the glucose uptake rate (modeled through the blue loop as a combination of internal and external effects). Altogether, these effects constitute a negative feedback loop aiming to reduce the flux entering the upper glycolysis if the processing capacity of the lower part is insufficient (feedback sense of the green loop). No distinction was

made here between upper and lower glycolysis and a single variable ϕ was considered. It is therefore assumed that the processing capacity of the glycolytic chain is similar to the uptake capacity, which eliminates the distinction between the upper and lower glycolysis and reduces the model complexity. A possible refinement can be sought in this direction, however, using the recent advances in this domain (Suarez-Mendez et al., 2017; van Heerden et al., 2014).

From a metabolic perspective, the mismatch between the cell demand and the environmental supply is the driving force of cell adaptation and metabolic adjustments. An outcome of our approach is that the ratio (actual uptake rate)/(actual growth rate) is not constant. The question of using a metabolic model to address the consequences of the mismatch between the substrate demand for growth and the actual uptake rate naturally arises from the above discussion. It was put aside in this work to focus on the model's dynamic behavior. However, the reader is invited to refer to our previous works where the metabolism of carbon excess/default with respect to the cell needs were addressed in detail (Pigou, 2018; Pigou & Morchain, 2015).

A major feature of biological systems, the existence of multiple uptake systems was not considered here. The very reason is that our model is a "relaxation-toward-steady-state model" and thus uses the steady-state uptake law as an attractor. Many studies proved that the apparent uptake rate results from numerous substrate transporters having their own concentration range of optimal efficiency (Ferenci, 1999; Liu & Ferenci, 1998; Postma et al., 1988; ter Kuile & Cook, 1994; Van Urk et al., 1989; Walsh et al., 1994). However, decades of experimental observations and recent results indicate that the apparent steady-state uptake rate is reasonably well described using a single Michaelis-Menten law, see fig. 1 in (Youk & van Oudenaarden, 2009). Our

model thus aims at describing the adaptation of the substrate import system, as a whole, without considering the dynamic switch and activation of these multiple uptake systems. This is certainly a major task to address in the future, and some elements can be found in (Quedeville, 2020)

5. Conclusion

A model describing the dynamics of the specific uptake rate in microbial cultures is proposed. The specific uptake capacity is made a property of the cell as was the growth capacity in previous works. The proposed model distinguishes between the cell capacities and the actual specific uptake and growth rates, which are determined from a comparison between the cell capacities and the supply from the environment. The uptake capacity evolves under the influence of two regulatory mechanisms aiming for a match between the uptake capacity and the environmental supply on the one hand and the uptake capacity and the cell's demand for growth on the other hand. An equilibrium is reached when the external supply, the uptake rate and the cell's demand are balanced. Thus, the dynamic model encompasses steady-state results and covers transient responses as well. Introducing the interfacial concentration as an unknown of the problem allows to describe external mass-transfer limitations of the actual bioreaction rates. A major conclusion is that there is no continuity of fluxes at the interface between liquid and biotic phases under transient conditions and thus may lead to substrate accumulation or deficit at the interface. A parametric study on the characteristic timescales of the different regulatory systems shows that a wide variety of experimental observations can be explained with this model. This simple model involving five differential equations decouples external mass transfer, uptake and growth rates in the transient regime. This feature seems to be crucial for the modeling of unsteady and/or heterogeneous bioreactors. Its extension to populational

approaches in combination with fluid transport is straightforward. However, accounting for multiple uptake systems working in parallel is needed to better describe short-term dynamics.

Acknowledgments

The authors gratefully acknowledge the financial support from the French National Research Agency through the 2015 "Attractivity Chair" program, Idex UNITI- "Biological, Reacting, Multiphase Flows (BIREM)" conv-ANR-11-Idex-0002-02.

References

Bailey, J. E., & Ollis, D. F. (1986). *Biochemical Engineering Fundamentals: Vol. Second* (K. Verma & C. Ce. Martin, Éds.). McGraw-Hill.

Brandman, O., Ferrell, J. E., Li, R., & Meyer, T. (2005). Interlinked Fast and Slow Positive Feedback Loops Drive Reliable Cell Decisions. *Science*, *310*(5747), 496. https://doi.org/10.1126/science.1113834

Ferenci, T. (1999). Regulation by nutrient limitation. *Current Opinion in Microbiology*, *22*(2), 208–213. https://doi.org/DOI: 10.1016/S1369-5274(99)80036-8

Gombert, A. K., & Nielsen, J. (2000). Mathematical modelling of metabolism. *Current Opinion in Biotechnology*, *11*(2), 180. https://doi.org/10.1016/S0958-1669(00)00079-3

Henson, M. A. (2003). Dynamic modeling of microbial cell populations. *Current Opinion in Biotechnology*, *14*(5), 460-467. https://doi.org/10.1016/S0958-1669(03)00104-6

Lambert, G., & Kussell, E. (2014). Memory and fitness optimization of bacteria under fluctuating environments. *PLOS Genetics*, *10*(9), e1004556. https://doi.org/10.1371/journal.pgen.1004556

Linkès, M., Fede, P., Morchain, J., & Schmitz, P. (2014). Numerical investigation of subgrid mixing effects on the calculation of biological reaction rates. *Chemical Engineering Science*, *116*, 473-485. https://doi.org/10.1016/j.ces.2014.05.005

Linkès, M., Martins Afonso, M., Fede, P., Morchain, J., & Schmitz, P. (2012). Numerical study of substrate assimilation by a microorganism exposed to fluctuating concentration. *Chemical Engineering Science*, *81*, 8-19. https://doi.org/10.1016/j.ces.2012.07.003

Liu, X., & Ferenci, T. (1998). Regulation of Porin-Mediated Outer Membrane Permeability by Nutrient Limitation in Escherichia coli. *Journal of Bacteriology*, *180*(15), 3917. https://doi.org/10.1128/JB.180.15.3917-3922.1998

Llaneras, F., & Picó, J. (2008). Stoichiometric modelling of cell metabolism. *Journal of Bioscience and Bioengineering*, *105*(1), 1-11. https://doi.org/10.1263/jbb.105.1

Maluta, F., Pigou, M., Montante, G., & Morchain, J. (2020). Modeling the effects of substrate fluctuations on the maintenance rate in bioreactors with a probabilistic approach. *Biochemical Engineering Journal*, *157*, 107536. https://doi.org/10.1016/j.bej.2020.107536

Merchuk, J. C., & Asenjo, J. A. (1995). The Monod equation and mass transfer. *Biotechnology and Bioengineering*, *45*(1), 91-94. https://doi.org/10.1002/bit.260450113

Morchain, J. (2017). *Bioreactor Modeling. Interactions between Hydrodynamics and Biology* (ISTE Press Ltd). London and Elsevier Ltd.

Morchain, J., & Fonade, C. (2009). A structured model for the simulation of bioreactors under transient conditions. *AIChE Journal*, *55*(11), 2973–2984. https://doi.org/10.1002/aic.11906

Morchain, J., Pigou, M., & Lebaz, N. (2017). A population balance model for bioreactors combining interdivision time distributions and micromixing concepts. *Biochemical Engineering Journal*, *126*(Supplement C), 135-145. https://doi.org/10.1016/j.bej.2016.09.005

Nielsen, J., & Villadsen, J. (1992). Modelling of microbial kinetics. *Chemical Engineering Science*, *47*(17-18), 4225-4270. https://doi.org/10.1016/0009-2509(92)85104-J

Palsson, B. Ø. (2011). *Systems Biology: Simulation of Dynamic Network States*. Cambridge University Press; Cambridge Core. https://doi.org/10.1017/CBO9780511736179

Pickett, A. M., Bazin, M. J., & Topiwala, H. H. (1979). Growth and composition ofEscherichia coli subjected to square-wave perturbations in nutrient supply: Effect of varying frequencies. *Biotechnology and Bioengineering*, *21*(6), 1043-1055. https://doi.org/10.1002/bit.260210609

Pigou, M. (2018). *Modélisation du comportement cinétique, des phénomènes de mélange, de transfert locaux et des effets d'hétérogénéité de population dans les fermenteurs industriels.* [PhD Thesis, Université de Toulouse, Institut National des Sciences Appliquées]. https://tel.archives-ouvertes.fr/tel-02917985

Pigou, M., & Morchain, J. (2015). Investigating the interactions between physical and biological heterogeneities in bioreactors using compartment, population balance and metabolic models. *Chemical Engineering Science*, *126*, 267-282. https://doi.org/10.1016/j.ces.2014.11.035

Postma, E., Scheffers, A. W., & Van Dijken, J. P. (1988). Adaptation of the Kinetics of Glucose Transport to Environmental Conditions in the Yeast Candida utilis CBS 621: A Continuous-culture Study. In *Microbiology,* (Vol. 134, Numéro 5, p. 1109-1116). Microbiology Society,.

Quedeville, V., Ouazaite, H., Polizzi, B., Fox, R. O., Villedieu, P., Fede, P., Létisse, F., & Morchain, J. (2018). A two-dimensional population balance model for cell growth including multiple uptake systems. *Chemical Engineering Research and Design*, *132*, 966-981. https://doi.org/10.1016/j.cherd.2018.02.025

Quedeville, Vincent. (2020). *Mathematical analysis, modelling and simulation of microbial population dynamics* [PhD dissertation, INP Toulouse]. http://www.theses.fr/2020INPT0033

Siebler, F., Lapin, A., Hermann, M., & Takors, R. (2019). The impact of CO gradients on C. ljungdahlii in a 125 m3 bubble column: Mass transfer, circulation time and lifeline analysis. *Chemical Engineering Science*, *207*, 410-423. https://doi.org/10.1016/j.ces.2019.06.018

Silveston, P. L., Budman, H., & Jervis, E. (2008). Forced modulation of biological processes: A review. *Chemical Engineering Science*, *63*(20), 5089-5105. https://doi.org/10.1016/j.ces.2008.06.017

Sonnleitner, B. (1998). Dynamic adaptation of microbes. *Measurement and Control*, *65*(1), 47-60. https://doi.org/10.1016/S0168-1656(98)00121-7

Sonnleitner, B., & Hahnemann, U. (1994). Dynamics of the respiratory bottleneck of Saccharomyces cerevisiae. *Journal of Biotechnology*, *38*(1), 63-79. https://doi.org/10.1016/0168-1656(94)90148-1

Sonnleitner, B., & Käppeli, O. (1986). Growth of Saccharomyces cerevisiae is controlled by its limited respiratory capacity: Formulation and verification of a hypothesis. *Biotechnology and Bioengineering*, *28*(6), 927-937. https://doi.org/10.1002/bit.260280620

Sonnleitner, B., Rothen, S. A., & Kuriyama, H. (1997). Dynamics of glucose consumption in yeast. *Biotechnology Progress*, *13*(1), 8-13. https://doi.org/10.1021/bp960094+

Suarez-Mendez, C. A., Ras, C., & Wahl, S. A. (2017). Metabolic adjustment upon repetitive substrate perturbations using dynamic (13)C-tracing in yeast. *Microbial Cell Factories*, *16*(1), 161-161. PubMed. https://doi.org/10.1186/s12934-017-0778-6

Sweere, A. P. J., Giesselbach, J., Barendse, R., de Krieger, R., Honderd, G., & Luyben, K. C. A. M. (1988). Modelling the dynamic behaviour of Saccharomyces cerevisiae and its application in control experiments. *Applied Microbiology and Biotechnology*, *28*(2), 116-127. https://doi.org/10.1007/BF00694298

Sweere, A. P. J., Luyben, K. Ch. A. M., & Kossen, N. W. F. (1987). Regime analysis and scale-down: Tools to investigate the performance of bioreactors. *Enzyme and Microbial Technology*, *9*(7), 386-398. https://doi.org/10.1016/0141-0229(87)90133-5

ter Kuile, B. H., & Cook, M. (1994). The kinetics of facilitated diffusion followed by enzymatic conversion of the substrate. *Biochimica et Biophysica Acta (BBA) - Biomembranes*, *1193*(2), 235-239. https://doi.org/10.1016/0005-2736(94)90158-9

van Heerden, J. H., Wortel, M. T., Bruggeman, F. J., Heijnen, J. J., Bollen, Y. J. M., Planqué, R., Hulshof, J., O'Toole, T. G., Wahl, S. A., & Teusink, B. (2014). Lost in transition: Start-Up of glycolysis yields subpopulations of nongrowing cells. *Science*, *343*(6174), 1245114. https://doi.org/10.1126/science.1245114

Van Urk, H., Postma, E., Scheffers, W. A., & Van Dijken, J. P. (1989). Glucose transport in crabtree-positive and crabtree-negative yeasts. In *Microbiology*, (Vol. 135, Numéro 9, p. 2399-2406). Microbiology Society,. https://doi.org/10.1099/00221287-135-9-2399

Walsh, M. C., Smits, H. P., Scholte, M., & van Dam, K. (1994). Affinity of glucose transport in Saccharomyces cerevisiae is modulated during growth on glucose. *Journal of Bacteriology, 176*(4), 953. https://doi.org/10.1128/jb.176.4.953-958.1994

Xiu, Z.-L., Zeng, A.-P., & Deckwer, W.-D. (1998). Multiplicity and stability analysis of microorganisms in continuous culture: Effects of metabolic overflow and growth inhibition. *Biotechnology and Bioengineering, 57*(3), 251-261. https://doi.org/10.1002/(SICI)1097-0290(19980205)57:3<251::AID-BIT1>3.0.CO;2-G

Youk, H., & van Oudenaarden, A. (2009). Growth landscape formed by perception and import of glucose in yeast. *Nature, 462*(7275), 875-879. https://doi.org/10.1038/nature08653

Young, T. B., Bruley, D. F., & H. R. Bungay, I. (1970). A dynamic mathematical model of the chemostat. *Biotechnology and Bioengineering, 12*(5), 747-769. https://doi.org/10.1002/bit.260120506

Zeng, A.-P., & Deckwer, W.-D. (1995). A kinetic model for substrate and energy consumption of microbial growth under substrate-sufficient conditions. *Biotechnology Progress, 11*(1), 71-79. https://doi.org/10.1021/bp00031a010

Figure 1: Time evolution of the model variables during a batch culture. The bottom right graph presents the imbalance between the external supply, the cell uptake capacity and the cell demand for growth. Balanced growth is characterized by the equality of these three variables.

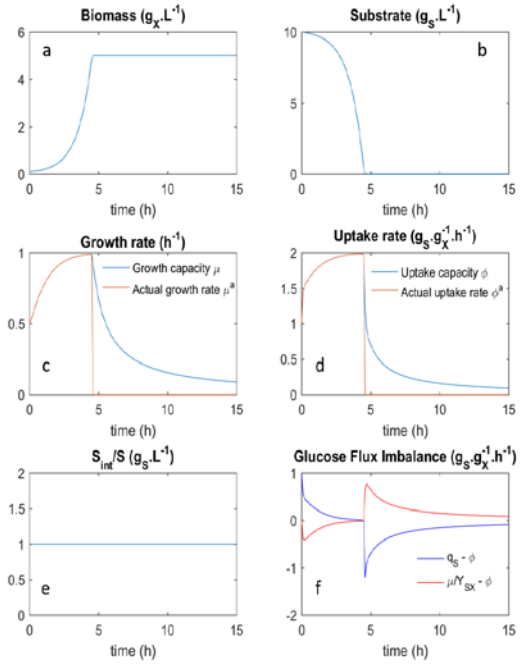

Figure 2: Time evolution of model variables toward steady state. Chemostat culture operated at $\boldsymbol{S_f = 10g.L^{-1}}$ and $\boldsymbol{D = 0.4\,h^{-1}}$. All parameters are identical to the batch simulation case, except $\boldsymbol{\tau_{\varphi,in} = 2.10^{-2}\,h}$, $\boldsymbol{\tau_{\varphi,ex} = 10^{-2}h}$.

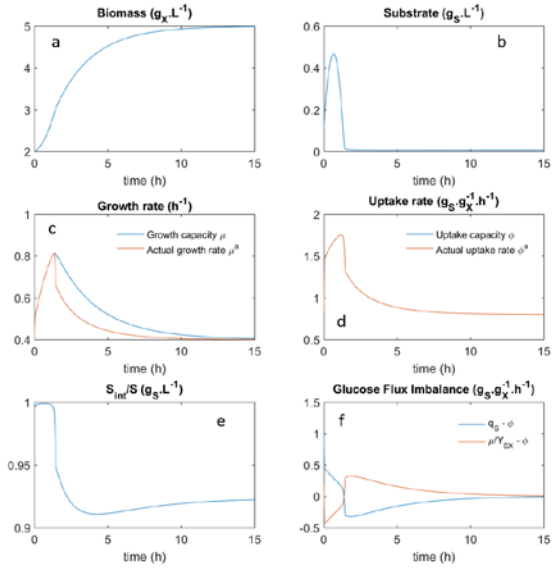

Figure 3: Time evolution of the substrate and biomass concentrations (a) and uptake capacity (b) following a dilution rate upshift from $\mathbf{0.25}$ to $\mathbf{0.5}\ \boldsymbol{h^{-1}}$. Various combinations of characteristic response times are presented. (a) The residual substrate concentration is highly sensitive to the characteristic times of the glycolytic chain regulation, while the biomass concentration is practically insensitive. (b) The group of lower curves represent the biological demand whereas the group of thinner curves in the upper part correspond to the supply from the environment.

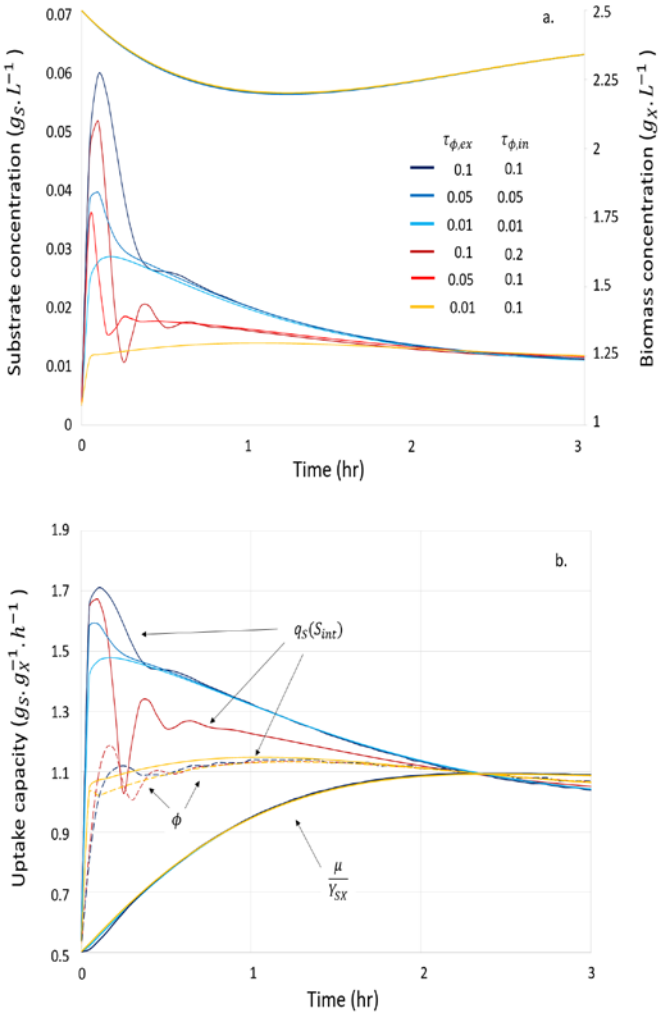

Figure 4: Time evolution of the model variables after a sudden drop down in the feed concentration at t=0. Chemostat culture initially performed at $D = 0.5\ h^{-1}$ and $S_f = 10\ g_S.L^{-1}$. The interfacial concentration plunges to zero whereas the actual uptake rate does remains positive. The actual uptake rate is controlled by external mass-transfer rate, which is lower than the uptake capacity in the first instants following the drop down in substrate.

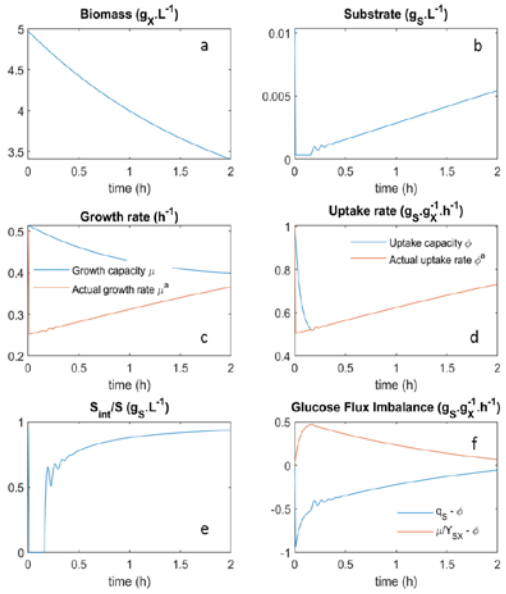

Figure 5: Time evolution of the residual glucose concentration during a dilution rate upshift $\mathbf{0.05}$ to $\mathbf{0.15}\ \boldsymbol{h^{-1}}$. Symbols: experimental data from (Sonnleitner et al., 1997), continuous line: simulated response. The parameters used for this simulation are reported in Table2.

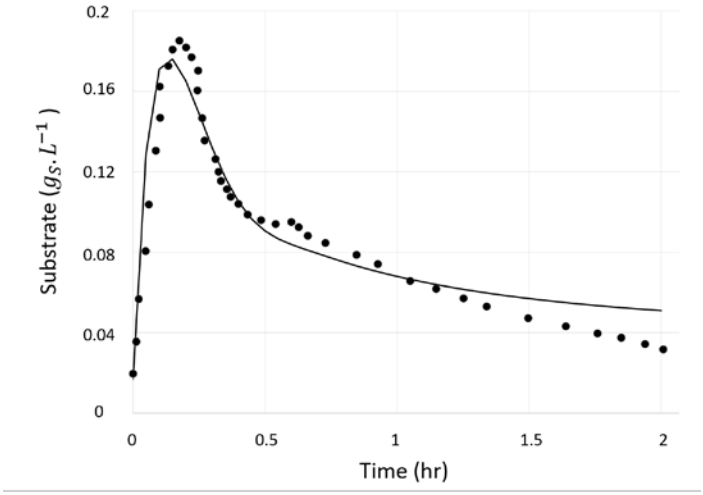

Figure 6: a. Time evolution of the residual glucose concentration during one feed cycle. b. Phase diagram: actual uptake rates and steady-state correlation as a function of the sugar concentration. Symbols: experimental data from (Suarez-Mendez et al., 2017), continuous line: simulated response, dashed line: steady-state correlation.

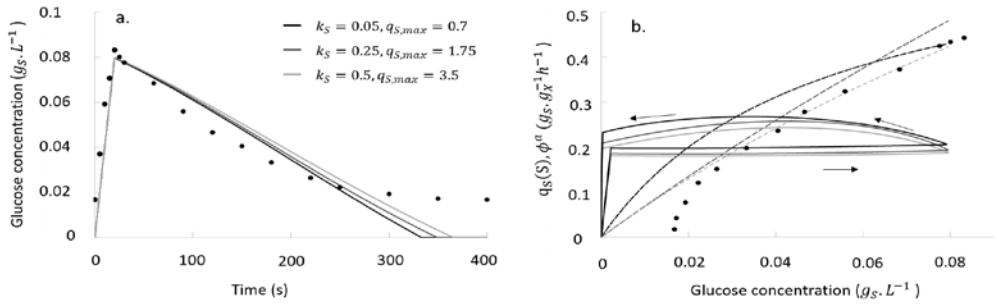

Figure 7: Dynamic phase portraits presenting the specific uptake and growth rate against the static uptake rate $q_S(S)$. Steady-state values are located on the steady-state line. Three typical trajectories are presented. External perturbation induces a deviation from this line and in the long term, each trajectory ends up on the steady-state line.

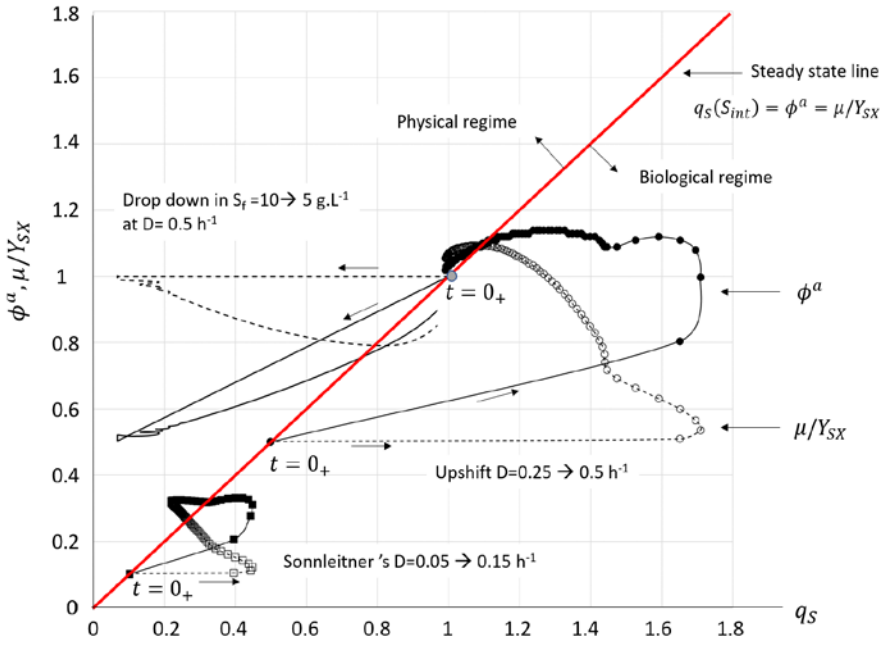

Figure 8: Scheme of the dynamic system using three regulatory loops. Continuous lines indicate that mass balances and operating conditions (S_f, D, τ_m) are involved. Dashed lines refer to intracellular regulation as considered in the model.

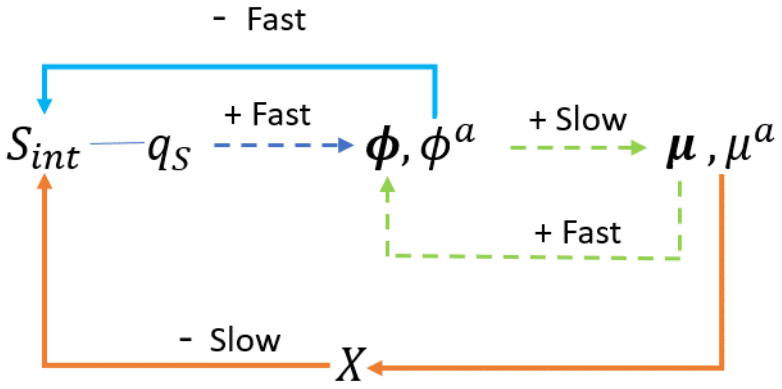

Table 1: Model parameters

Table 2: Model parameters for the simulation of the experimental data of Sonnleitner

Appendix A: Model simplification under the assumption that regulatory mechanisms share the same characteristic time

If one introduces the assumption that the two timescales in equation (7) are identical, one gets

$$\frac{d\phi}{dt} = \frac{1}{\tau_\phi}\left(\left(\frac{\mu}{Y_{SX}} + q_{S,max}\frac{S_{int}}{k_S+S_{int}}\right) - 2\,\phi\right) \quad (14)$$

and equation (27) may be used in place of equation (7).

Equation (27) also writes

$$\frac{d\phi}{dt} = \frac{2}{\tau_\phi}(\phi^* - \phi) \quad (15)$$

$$\phi^* = \frac{1}{2}\left(\frac{\mu}{Y_{SX}} + q_{S,max}\frac{S_{int}}{k_s+S_{int}}\right) \quad (16)$$

with the following definition for ϕ^*

In this form, it is visible that the model describes the adaptation of the glucose uptake capacity toward the arithmetic mean of the external supply and the internal demand. This resembles the empirical correlation for the uptake rate, as exposed by Zeng in a series of work in the 1990's (Xiu et al., 1998; Zeng & Deckwer, 1995) and formerly used in our previous work without any theoretical justification (equation 2.12 in (V. Quedeville et al., 2018)).

However, the fundamental originality of the present work is that ϕ^* acts here as an "attractor" for ϕ whereas it was considered in previous works as a direct estimate for the actual uptake rate.

Appendix B: Comparison of the model predictions with experimental data

Operating conditions and model parameters are listed in Table 2. It was reported by the authors of the experiments that they took care to avoid oxygen limitation. They also choose to operate at a low dilution rate to prevent autonomous oscillations of the yeast culture and to prevent a possible metabolic shift in the oxydo-reductive region ($D > 0.35\ h^{-1}$). In practice the only parameters that require an effort for the fit were the maximum uptake rate and the affinity constant for the substrate. We did not

consider the maximum substrate uptake rate typically reported for *Saccharomyces cerevisiae* (3.5 $g_S.g_X^{-1}.h^{-1}$) because this maximum is observed when both oxidative and reductive metabolism are present (above $D > 0.35\,h^{-1}$). Also, Sonnleitner's works indicate that the respiratory bottleneck is not responsible for the observed change in the consumption rate (Sonnleitner et al., 1997; Sonnleitner & Hahnemann, 1994). We set the maximum uptake rate to the maximum value in the oxidative mode, observed below $D = 0.35$, leading to $q_{S,max} = 0.7\ g_S.g_X^{-1}.h^{-1}$. This suggests that multiple transport systems are responsible for the glucose uptake, a common feature of biological systems as evidenced by many studies on yeasts or bacteria (Ferenci, 1999; Van Urk et al., 1989; Walsh et al., 1994). It can be thought that the saturation of the absolute maximum oxidative capacity of the yeast promotes the activation of an additional uptake system allowing the maximum uptake rate to reach a higher value if needed.